

STATUS REPORT 2

PROJECT TITLE: LOCAL AND GLOBAL ACOUSTIC CONTROL FOR LAUNCH VEHICLE PAYLOAD FAIRINGS

INVESTIGATOR: DR. DONALD J. LEO
CIMSS / MECHANICAL ENGINEERING DEPARTMENT
310 NEW ENGINEERING BLDG.
VIRGINIA TECH
BLACKSBURG, VA, 24061-0261

TEL: (540) 231-2917
FAX: (540) 231-2903
EMAIL: donleo@vt.edu

PURCHASE ORDER: 00-04-6838

START DATE: 10-MAY-00
END DATE: 09-MAY-00

ACCOMPLISHMENTS SINCE PREVIOUS PROGRESS REPORT:

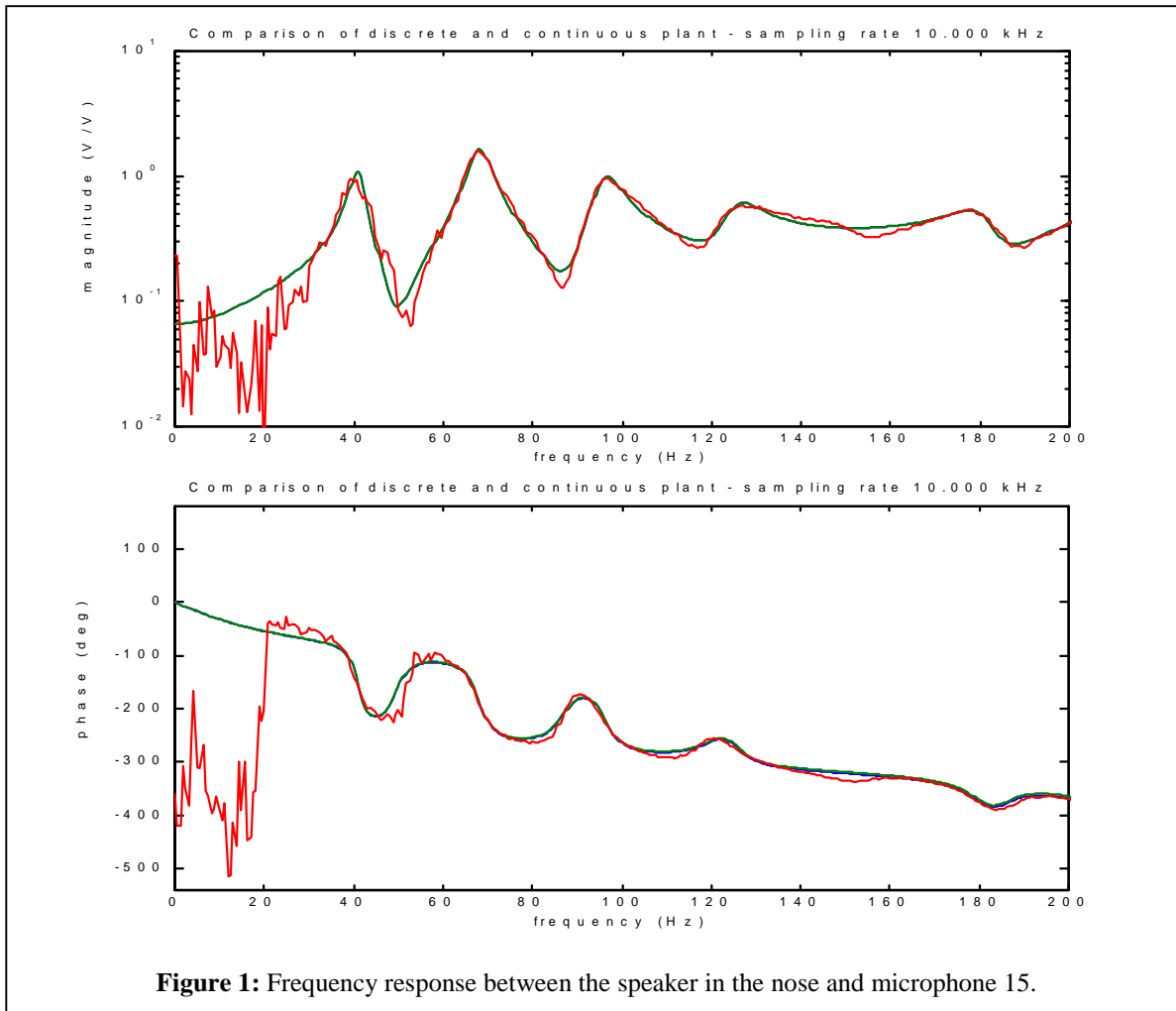
1. Traveled to Duke University (Dr. Don Leo, Kevin Farinholt – VT, Dr. Steve Griffin – AFRL) to perform feedback control experiments on the fairing test article located in Dr. Robert Clark's facility.
2. Demonstrated through experiment that global noise attenuation is possible using a single control source and a single microphone. Experimental results demonstrated a 1.6 dB RMS reduction (0-200 Hz) and a 5 dB peak reduction in the spatially-averaged frequency response.

Objective:

The objective of the control experiments is to demonstrate the ability of single-input-single-output feedback control to provide global noise attenuation in the fairing cavity. Global noise attenuation is defined as the reduction in RMS (or peak) sound pressure at multiple locations within the fairing. Global attenuation contrasts with *local* attenuation in which only a finite region near the control source is controlled, resulting in negligible attenuation (or possibly amplification) of the sound pressure levels at other locations within the fairing.

Control Modelling:

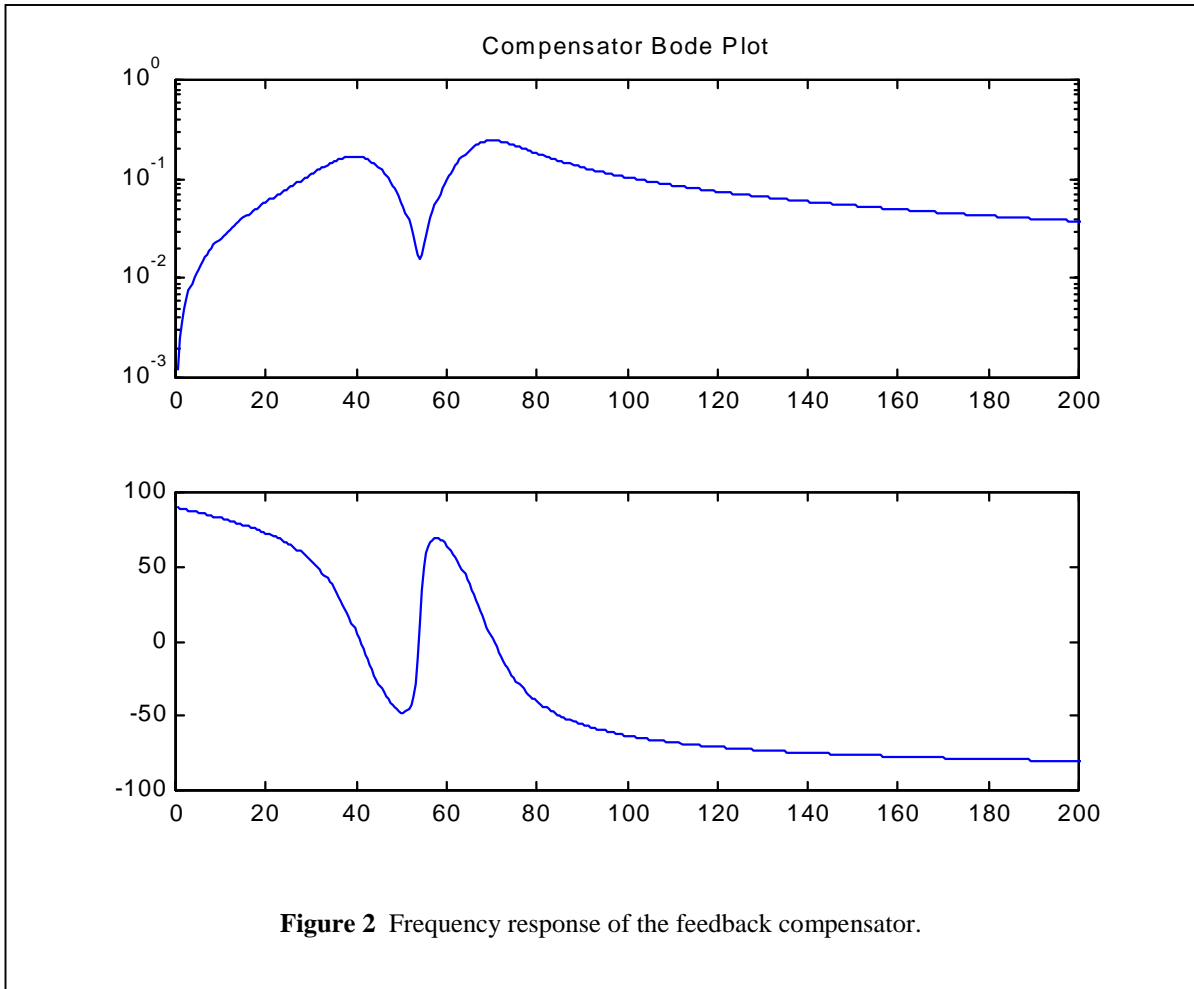
The control source is chosen to be the speaker in the nose of the fairing and the feedback sensor is chosen to be a microphone at location 15. The distance between the source and the sensor is approximately 2 feet. This sensor-actuator pair is chosen so that the pole-



zero spacing will be increased as compared to the microphone located directly in front of the speaker in the nose.

Frequency response data is obtained over the frequency range 0-2 kHz for this sensor-actuator pair. The bandwidth of the frequency response is high compared to the control bandwidth (\sim 0-200 Hz) so that the state-space identification of the system dynamics will accurately account for out-of-band dynamics. The acoustic damping in the fairing is substantial due to the 7.5 cm (3 in.) thick absorber lining placed on the walls of the cavity. The phase lags associated with the resonant modes above 200 Hz must be included in the data set to produce an accurate state-space representation of control transfer function.

The frequency response between the noise speaker and microphone 15 is shown in Figure 1. A 40-state continuous-time state-space model is identified using the Eigensystem Realization Algorithm (ERA) implemented in the Matlab function EZERA.M. Figure 1 illustrates that the identified model accurately represents the experimental data over the frequency range 0-200 Hz.



The control transfer function exhibits the pole-zero interlacing associated with a ‘collocated’ sensor-actuator pair. The first phase reversal occurs in the fifth resonant mode at approximately 180 Hz. The modes exhibit approximately 4% critical damping due to the energy dissipation associated with the sound absorbing material on the inner wall of the fairing. The gradual phase lag exhibited in the bottom plot of Figure 1 is associated with the highly-damped resonances above 200 Hz.

Control Design:

Feedback control is achieved with a compensator designed to dissipate energy in the first two resonances of the fairing cavity. The compensator is of the form

$$K(s) = \sum_{i=1}^N \frac{(as + b)\omega_f^2}{s^2 + 2\zeta_f\omega_f s + \omega_f^2} \tag{1}$$

where a , b , ζ_f , and ω_f are control parameters. If a is zero then this compensator is simply a positive position feedback filter; setting $b = 0$ results in a filtered strain rate feedback compensator. Compensators of this form are designed by including one control filter for each resonance. The design procedure is to vary the filter parameters such that the loop

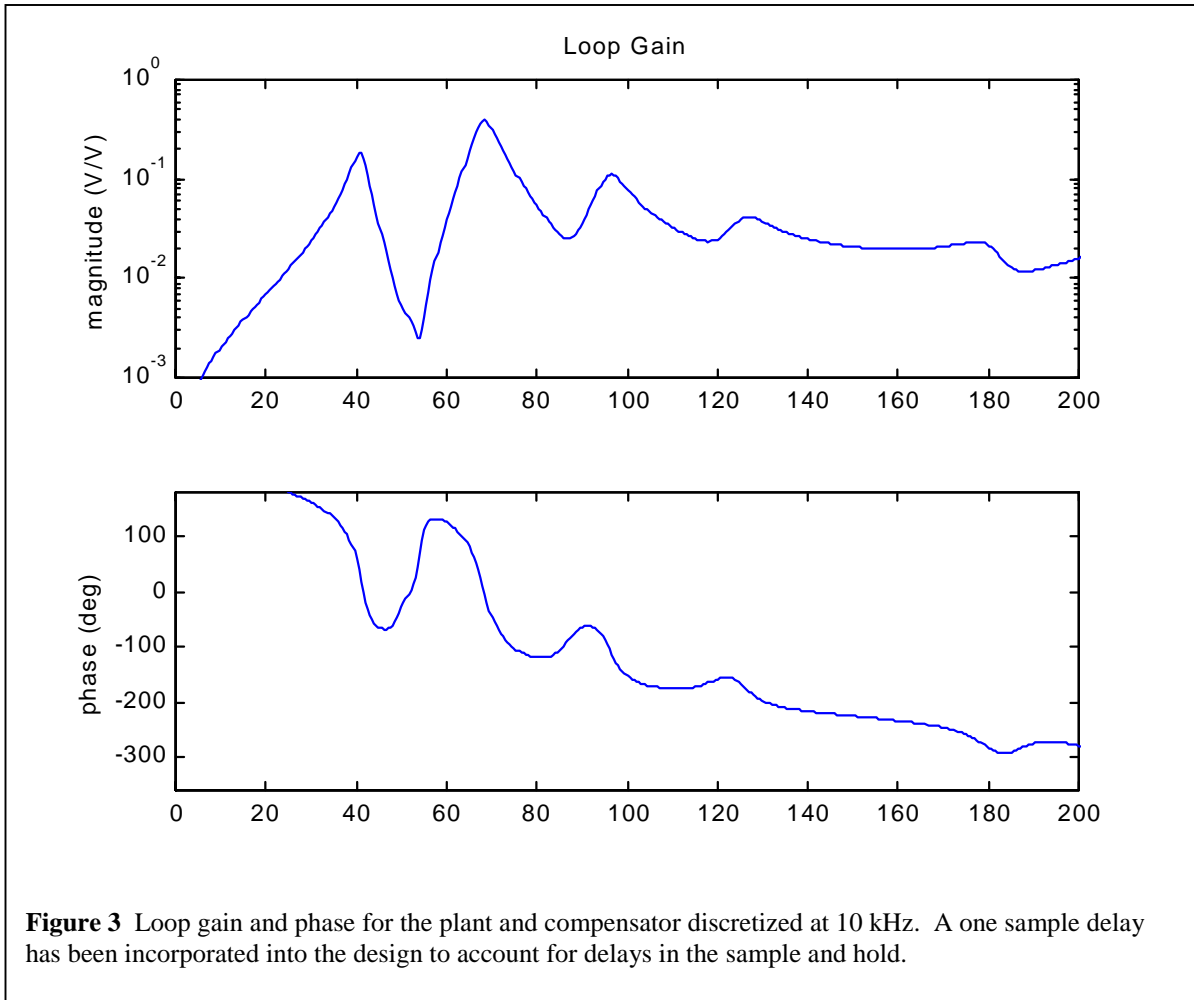


Figure 3 Loop gain and phase for the plant and compensator discretized at 10 kHz. A one sample delay has been incorporated into the design to account for delays in the sample and hold.

transfer function is positive real near the target resonances. A positive real transfer function near resonance will result in energy dissipation in the resonance and a migration of the pole further into the left-half plane. Increasing the energy dissipation in the resonance provides global attenuation due to the fact that the amplification due to resonance is decreased at all points within the cavity.

Figure 2 is a plot of the compensator frequency response. The parameters of the compensator are chosen to produce a loop gain with approximately zero phase near the first two resonances of the cavity.

The fourth-order compensator is discretized at 10 kHz for digital implementation. Figure 3 is a plot of the loop gain using a discrete model of the plant in series with a discrete model of the compensator. A one-sample delay has been included in the discretization to account for delays in the sample and hold. The loop phase illustrates that the phase is approximately zero degrees near resonance of the first two modes, 40 Hz and 68 Hz, respectively.

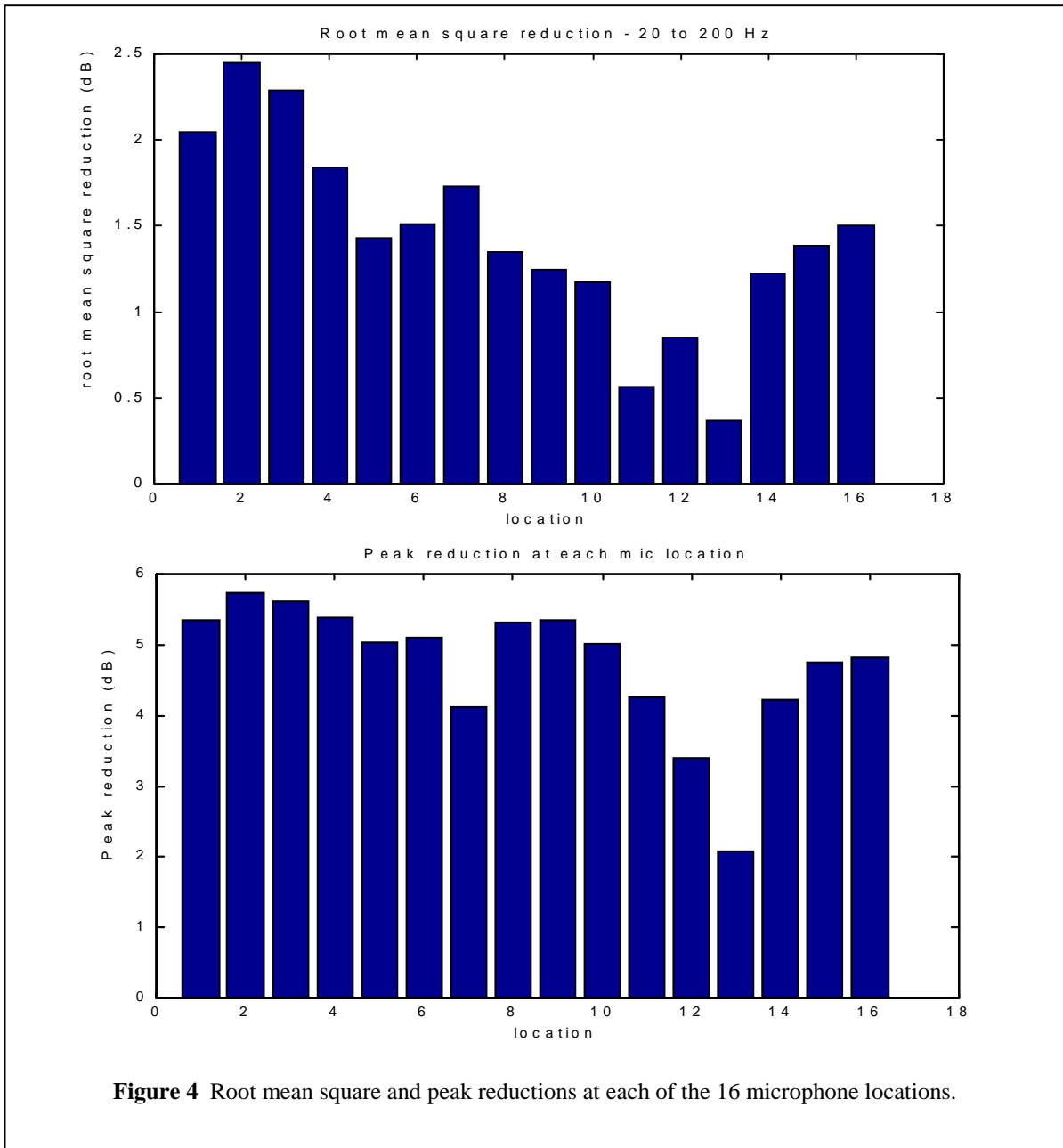


Figure 4 Root mean square and peak reductions at each of the 16 microphone locations.

Control Results

Open- and closed-loop frequency responses are obtained between the disturbance speaker and the microphones within the fairing. The root mean square response at the microphone location to a white noise disturbance is computed from the expression

$$RMS = \left[\int_{f_1}^{f_2} |H_{ij}(jf)|^2 df \right]^{1/2} \quad (2)$$

where H_{ij} is the transfer function between the disturbance speaker and the microphone. The peak response of at each microphone location is also determined.

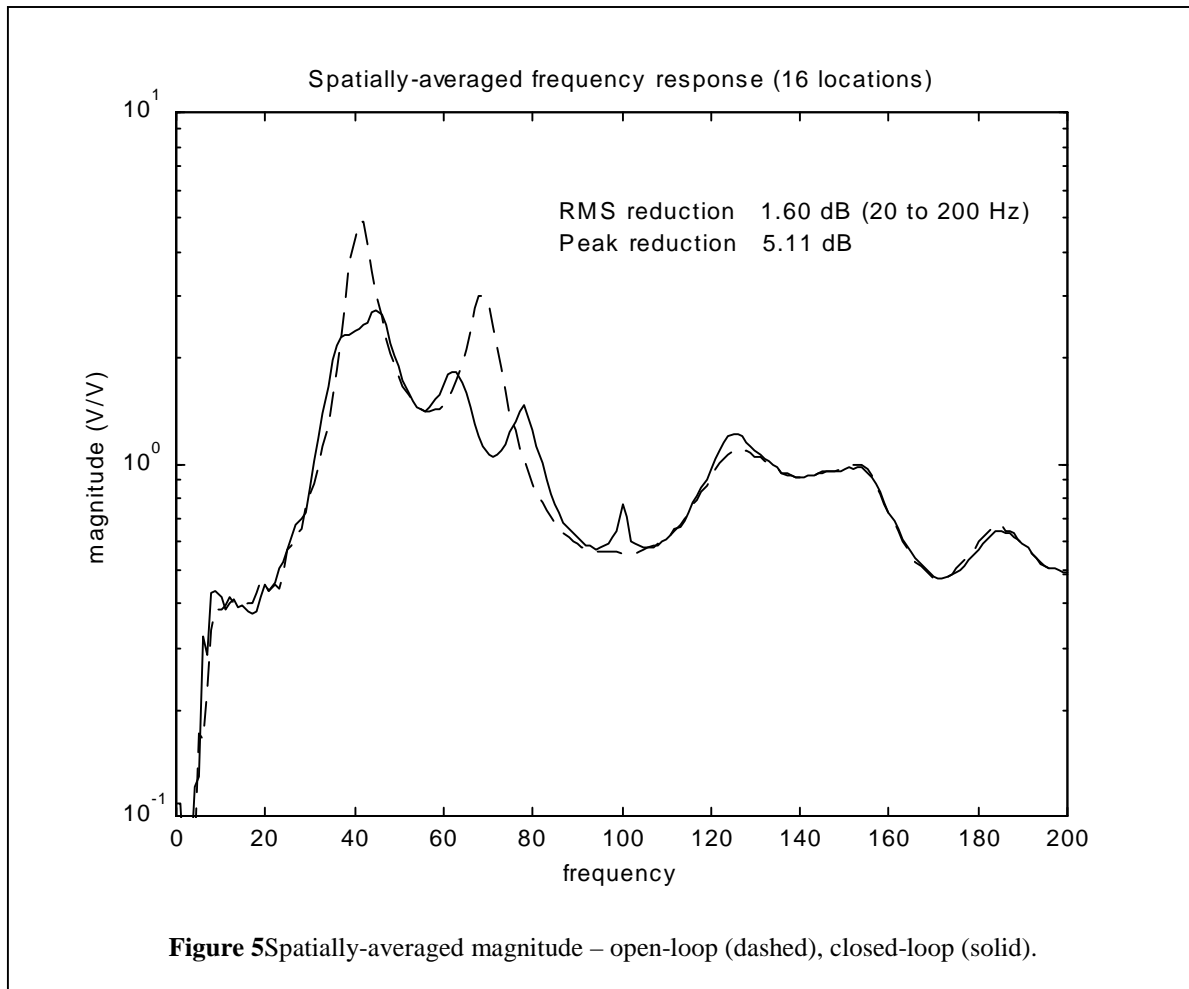


Figure 4 is a comparison of the RMS reduction and peak reduction at each of the 16 microphone locations. The RMS reduction is calculated between 20 and 200 Hz to eliminate errors due to low-frequency noise in the data. The fact that the RMS level is being reduced at all microphone locations demonstrates that global attenuation is being achieved. Three locations exhibit a 2 dB reduction or greater, ten locations exhibit between 1 and 2 dB, and three locations exhibit less than a 1 dB attenuation. Peak reductions are approximately 5 dB at most locations within the cavity.

The spatially-averaged response magnitude is computed using the results of the 16 transfer function tests. Figure 5 is a plot of the spatially-averaged magnitude for open-loop with an absorptive trim and closed-loop. The magnitude demonstrates that the feedback compensator is able to decrease the resonant amplification at the first two modes of the fairing. This is attributed to the active damping introduced by the compensator. The average RMS reduction is 1.6 dB (17% -- 20 to 200 Hz) and the peak reduction is 5.1 dB. Control spillover occurs in the 100 – 120 Hz frequency range due to the limited phase margin at these frequencies (see Figure 3).

UPCOMING TASKS:

1. Explore sequential loop closing as a means of increasing energy dissipation in the acoustic resonances.
2. Quantify the coupling between the control source and the cavity with a model of a tapered waveguide.
3. Quantify the benefits associated with increased coupling between the control source and the cavity resonances.